

See discussions, stats, and author profiles for this publication at: <https://www.researchgate.net/publication/261880432>

# Intramolecular Charge Transfer Effects on the Diradical Character and Second Hyperpolarizabilities of Open-Shell Singlet $X-\pi-X$ ( $X$ = Donor/Acceptor) Systems

ARTICLE in THE JOURNAL OF PHYSICAL CHEMISTRY A · APRIL 2014

Impact Factor: 2.69 · DOI: 10.1021/jp412634q · Source: PubMed

---

CITATIONS

8

---

READS

35

2 AUTHORS, INCLUDING:



Masayoshi Nakano

Osaka University

337 PUBLICATIONS 4,785 CITATIONS

SEE PROFILE

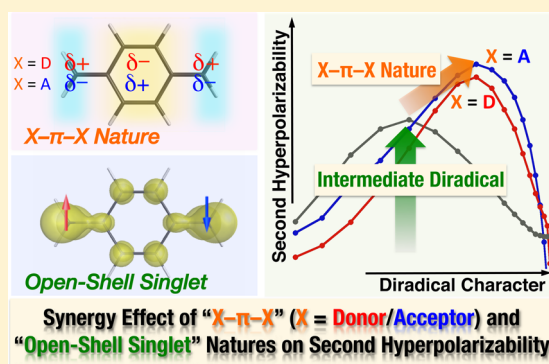
# Intramolecular Charge Transfer Effects on the Diradical Character and Second Hyperpolarizabilities of Open-Shell Singlet $X-\pi-X$ ( $X = \text{Donor/Acceptor}$ ) Systems

Kotaro Fukuda and Masayoshi Nakano\*

Department of Materials Engineering Science, Graduate School of Engineering Science, Osaka University, Toyonaka, Osaka 560-8531, Japan

## S Supporting Information

**ABSTRACT:** We investigate the effect of the quadrupole-type intramolecular charge transfer (ICT) in open-shell singlet donor- $\pi$ -donor ( $D-\pi-D$ ) molecules on the singlet open-shell (diradical) character and the longitudinal second hyperpolarizabilities  $\gamma$  (the third-order nonlinear optical (NLO) properties at the molecular scale). For this investigation we used the *para*-quinodimethane (PQM) with point charges (pc's) model calculated with the unrestricted coupled cluster method including single and double excitations with a perturbative treatment of the triple excitations (UCCSD(T)). In this model, the diradical character  $y$  and the amount of the ICT, that is, the  $D-\pi-D$  nature, can be varied primarily by changing the exocyclic carbon-carbon bond (C-C) lengths and the external pc's  $Q$ , respectively. It turns out that the increase in the  $D-\pi-D$  nature decreases the  $y$  values, moves the  $y$  values ( $y_{\max}$ ) giving the maximum  $\gamma$  ( $\gamma_{\max}$ ) to the large  $y$  region, and enhances the  $\gamma_{\max}$  values, for example, the  $\gamma_{\max}$  of the singlet diradical PQM with  $Q = -2.8$  au reaches twice that of the singlet diradical PQM without any pc's. This result indicates that open-shell singlet  $D-\pi-D$  systems with ICT are promising candidates for a new class of third-order NLO molecules, whose  $\gamma$  values are more enhanced than those of conventional closed-shell  $D-\pi-D$  systems and of symmetric open-shell singlet systems without the ICT. To confirm this tendency, we examine the boron-disubstituted PQM dianion model, which is found to exhibit further enhancement of  $\gamma$  as compared to the PQM model with intermediate diradical character due to the synergy effects of the intermediate open-shell singlet nature and the strong field-induced ICT nature in the dianionic state of the  $D-\pi-D$  system. Further investigation of the acceptor- $\pi$ -acceptor ( $A-\pi-A$ ) type ICT effect in the PQM-pc model shows that both  $D-\pi-D$  and  $A-\pi-A$  type symmetric ICTs give similar effects on the relationship between  $y$  and  $\gamma$ , though there are some differences originating in the orbital contraction and extension induced by the pc's. The present results contribute to understanding the third-order NLO properties of open-shell symmetric ICT systems and thus to constructing new design guidelines for highly efficient third-order NLO systems.



## 1. INTRODUCTION

The molecular design for novel nonlinear optical (NLO) systems has been extensively explored because of their potential applications in future photonics and optoelectronics such as ultrafast optical switching,<sup>1</sup> high-capacity three-dimensional memory,<sup>2</sup> three-dimensional microfabrication,<sup>3</sup> efficient optical limiting,<sup>4</sup> and photodynamic therapy.<sup>5</sup> Until now, several molecular design guidelines for realizing large NLO properties have been presented, for example, tuning the structure and size of  $\pi$ -conjugated linkers,<sup>6</sup> donor or acceptor substitutions,<sup>7-9</sup> and charging.<sup>10</sup> Among them, the introduction of quadrupole-type symmetric intramolecular charge transfer (ICT) induced by the substitution of electron-donor or -acceptor moieties to both sides of the molecular skeleton is a well-known design guideline.<sup>7-9</sup> In the illustrative studies on bis(styryl)benzene derivatives,<sup>7,8</sup> it was found that several symmetric bis(styryl)-benzene derivatives with electron-donating or -accepting end groups exhibit exceptionally large two-photon absorption

(TPA), which is a typical third-order NLO property as compared to the systems without donor or acceptor groups. Such a significant enhancement of the third-order NLO property is found to be caused by the increase of the transition moment amplitude between the excited states originating from the symmetric ICT. On the basis of the relationship between the NLO property and the ICT, several real molecular systems with large third-order NLO properties have been designed.<sup>9</sup>

On the other hand, open-shell singlet systems have recently attracted much attention as a new class of highly efficient NLO systems, based on our theoretical prediction<sup>11-25</sup> of a strong correlation between the diradical character  $y$ <sup>26-30</sup> and the second hyperpolarizability  $\gamma$ , which is an origin of the third-order NLO property at the molecular level.<sup>31-46</sup> The diradical

Received: December 26, 2013

Revised: April 2, 2014

Published: April 24, 2014



character is a well-defined index of open-shell singlet nature in quantum chemistry that takes a value between 0 (closed-shell) and 1 (pure open-shell). The origin of the  $\gamma$ - $\gamma$  correlation has been clarified based on the valence configuration interaction (VCI), the symmetric or asymmetric two-site diradical models,<sup>12–16</sup> and the full-configuration-interaction linear  $H_4$  model.<sup>17</sup> To reveal the structure–NLO property relationships based on the  $\gamma$ - $\gamma$  correlation, we have also examined  $\gamma$  and  $\gamma$  values for the *para*-quinodimethane (PQM) model,<sup>11</sup> metal–metal multiple bonded systems,<sup>18,19</sup> and main group compounds.<sup>20</sup> It turns out that PQM with the equilibrium geometry exhibits a finite small singlet diradical character ( $\gamma \approx 0.15$  at the spin-projected unrestricted Hartree–Fock (PUHF) level of approximation) since PQM possesses two resonance structures, that is, closed-shell quinoid and open-shell benzenoid structures. By examining a PQM model by varying the exocyclic carbon–carbon (C–C) bond length  $r$ , it was found that the diradical character  $\gamma$  increases when  $r$  increases, and the longitudinal  $\gamma$  value attains a maximum in the intermediate  $\gamma$  region. Namely, molecules including the contribution of quinoid and benzenoid resonance structures are expected to be potential candidates for diradicaloids, which present intermediate  $\gamma$  values and thus exhibit large  $\gamma$  values. On the basis of this design principle, we have investigated several realistic open-shell singlet systems, for example, diphenalenyl diradicaloids<sup>21</sup> and graphene nanoflakes.<sup>22–25</sup> Later, huge two-photon absorption cross sections<sup>40–44</sup> and third harmonic generation<sup>45,46</sup> were observed in various singlet diradical systems with intermediate  $\gamma$  values, the facts of which have confirmed the validity of our theoretical predictions.

As a further exploration direction of new NLO molecular design guidelines, in this study we investigate a synergy effect between the two guidelines previously mentioned, that is, a significant quadrupole-type symmetric ICT and the intermediate open-shell singlet character. Namely, the  $\gamma$  enhancement effect by the quadrupole-type ICT, for example, donor– $\pi$ –donor (D– $\pi$ –D) nature, for open-shell singlet systems with different  $\gamma$  values is investigated using the modified PQM model. By putting external negative point charges (pc's) on the original PQM model,<sup>11</sup> we can model after the open-shell singlet systems with the ICT induced by, for example, introducing donor groups with radical natures into the *para*-positions. The open-shell nature and the degree of ICT can be varied primarily by changing the exocyclic C–C bond length, and by tuning the position, sign, and the amount of the external pc's, respectively. To verify the tendencies obtained by the PQM with pc's (PQM-pc) model, we examine the boron (B)-disubstituted PQM dianion model, where the D– $\pi$ –D nature is expected without any external pc's, while the open-shell nature can be varied with the exocyclic C–B bond length. We also perform the investigation of the acceptor– $\pi$ –acceptor (A– $\pi$ –A) effect in the PQM-pc models with a positive pc of +2.0 au and discuss the similarity and difference between the D– $\pi$ –D and A– $\pi$ –A systems. On the basis of these results, we present a new design guideline for the X– $\pi$ –X (X = D/A) open-shell singlet systems, which are expected to exhibit more enhanced  $\gamma$  values than conventional closed-shell X– $\pi$ –X (X = D/A) systems and open-shell singlet systems without the ICT.

## 2. METHODOLOGY

**2.1. Model Systems.** Figure 1 shows the geometry and the resonance structures of the PQM model (Figure 1a and Figure 1b). The PQM model possesses two resonance structures, that

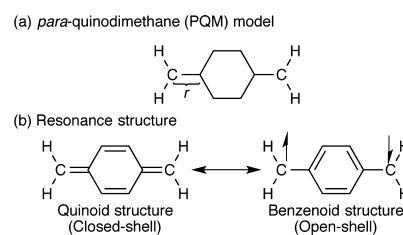


**Figure 1.** Molecular framework (a) and resonance structures (b) of the PQM model.

is, closed-shell quinoid and open-shell diradical structures, where the contribution of the diradical form is related to the singlet open-shell character of this system in the ground state. As shown in our previous study,<sup>11</sup> the ground state of the PQM presents an almost quinoid structure and the variation in the exocyclic C–C bond length  $r$  causes a wide range of variation in the diradical character. Indeed, it has been revealed that the larger  $r$  value corresponds to the dissociation of the exocyclic C–C  $\pi$ -bonds, showing the increase in the diradical character. In this study, the PQM structures are optimized with each fixed  $r$  value ranging from 1.35 to 2.20 Å, under the constraint of  $D_{2h}$  symmetry.

Figure 2 shows the PQM-pc model, which is the main concern in this study. Two pc's are placed a few Å away from

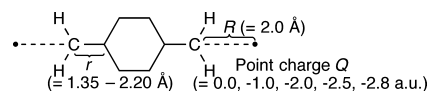


**Figure 2.** Structure of the PQM-pc model. The  $r$  and  $R$  values indicate the exocyclic C–C bond length and the distance between the exocyclic C atoms and pc's, respectively.

each exocyclic C atom along the longitudinal axis, where these external charges cause the ICT within the PQM and thus lead to the emergence of the dipole or the quadrupole-type charge distribution. The charge distribution in the PQM is predicted to be tuned by varying the amount of pc's  $Q$  or the distance  $R$  between the exocyclic C atoms and the pc's, for example, adopting larger pc's is expected to induce a larger ICT. In addition, as indicated previously, the variation in the exocyclic C–C bond length is predicted to cause the variation in the open-shell singlet nature of the PQM. The PQM-pc model is thus useful for investigating the ICT effects on the open-shell singlet systems with different diradical characters. In this study, we focus on the system with symmetric quadrupole D– $\pi$ –D type charge distribution, which is realized by mutually adopting the same negative  $Q$  values ( $= 0.0, -1.0, -2.0, -2.5$ , and  $-2.8$  au) on both sides of the system with the fixed distance  $R = 2.0$  Å between the exocyclic C atoms and the pc's. These different  $Q$  values are found to vary the D– $\pi$ –D nature. The geometry of PQM is optimized at each  $r$  value without pc's. We neglect the effect of the pc's on the geometric change in this model since we aim to obtain qualitative relationships between the ICT effects, diradical character, and  $\gamma$  values. The geometry optimizations for each  $r$  value (ranging from 1.35 to 2.20 Å) are performed using the spin–flip (SF) time-dependent density functional theory (TDDFT) with the Tamm–Dancoff approximation together with the collinear approximation with the BHandHLYP functional,<sup>47</sup> which is found to well reproduce the geometries of open-shell singlet hydrocarbons.<sup>48</sup> The

extended basis set, 6-31G\*+*p*, with a diffuse *p* exponent of 0.0523 for C atoms and 0.0447 for B atoms, is employed.<sup>49</sup>

**2.2. Diradical Character of the PQM Model without pc's.** Here we examine the variation in the diradical character of the model system without pc's, which is identical to the original PQM model<sup>11</sup> except for the molecular geometries. Following our previous studies,<sup>11,18,19,21–23</sup> the PUHF scheme is employed for the calculation of the diradical character,<sup>27</sup> which is originally defined as twice the weight of the doubly excited configuration in the ground state.<sup>28</sup> Within the PUHF scheme, the diradical character is expressed as<sup>27</sup>

$$y = 1 - \frac{2T}{1 + T^2} \quad (1)$$

where *T* is the orbital overlap between the HOMO and LUMO and also can be represented by using the occupation numbers (*n<sub>i</sub>*) of UHF natural orbitals (UNOs) as<sup>27</sup>

$$T = \frac{n_{\text{HOMO}} - n_{\text{LUMO}}}{2} \quad (2)$$

The diradical character *y* takes a value between 0 and 1, which indicates the closed-shell and pure diradical states, respectively. Figure 3 shows the variation in *y* as a function of

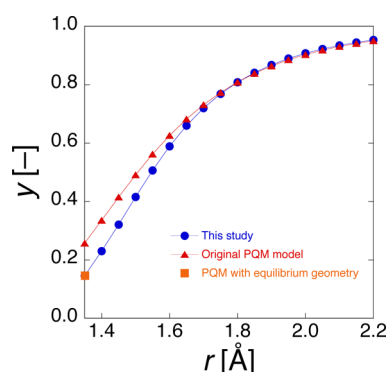


**Figure 3.** Variation in the diradical character *y* as a function of the exocyclic C–C bond length *r* for the present and the original PQM models calculated using the PUHF/6-31G\*+*p* method.

the exocyclic C–C bond length for the present and previous models.<sup>11</sup> It was found that the *y* values of the present model monotonically increase with the increase in the exocyclic C–C bond length *r*, and that this tendency qualitatively agrees with the original PQM model, which employs a fixed geometry of the central benzene ring (C–C bond length = 1.4 Å) regardless of the *r* value. It was also found that the *y* values of the original PQM model are slightly larger than those of the present model, in particular, in the small *r* region. This is understood by the fact that the original PQM model neglects the bond length alternation (BLA) of the central benzene ring, the feature of which leads to more contribution of the diradical resonance structure shown in Figure 1b.

**2.3. Charge Transfer in the PQM-pc Model with the Exocyclic C–C Bond Length *r* = 1.35 Å.** We evaluate the charge distribution using the natural population analysis with the UHF calculation, which is sufficient for the present purpose as seen from the comparison of the results obtained by different population analysis schemes with UHF calculations and by the same population analysis scheme with strong electron-correlated calculations (see Figure S1 in the Supporting Information). To evaluate the degree of the D–π–D nature

for each system, we examine the summation of the natural charge of each atom in the central benzene ring ( $\Delta q$ ), where the system with larger  $-\Delta q$  value indicates a larger charge transfer from the D(CH<sub>2</sub>) groups to the central benzene ring, that is, a stronger D–π–D nature. Figure 4 shows the variation

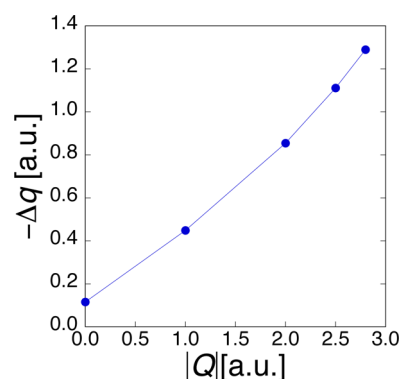


**Figure 4.** Variation in the ICT from the D(CH<sub>2</sub>) groups to the central benzene ring ( $-\Delta q$ ) as a function of the magnitude of pc  $|Q|$  ( $Q = 0.0, -1.0, -2.0, -2.5$ , and  $-2.8$  au) of the PQM-pc model with a fixed exocyclic C–C bond length  $r$  (= 1.35 Å) calculated using the UHF/6-31G\*+*p* method.

in the ICT as a function of  $|Q|$  for the PQM-pc model with a fixed  $r = 1.35$  Å, which is almost equal to the  $r$  value of the equilibrium structure ( $r_{\text{eq}} = 1.348$  Å). It was found that the amount of the charge transfer  $-\Delta q$  is quite small (0.12 au) at first in the absence of pc's, while the increase in the magnitude of external pc  $|Q|$  increases the  $-\Delta q$  value, which shows almost a linear dependence on  $|Q|$ . More details of the natural charge value for each atom are given in Table 1 in the cases of  $Q = 0.0$

**Table 1.** Natural Charge (au) of Each Symmetry-Unique Atom in the Case of  $Q = 0.0$  and  $-2.0$  au Calculated with the UHF/6-31G\*+*p* Method

		$Q = 0.0$ au	$Q = -2.0$ au
terminal CH <sub>2</sub> region	C <sub>1</sub>	−0.346	−0.134
	H <sub>1</sub>	0.202	0.281
central benzene region	C <sub>2</sub>	−0.107	−0.296
	C <sub>3</sub>	−0.200	−0.242
	H <sub>2</sub>	0.224	0.176

au and  $-2.0$  au. Although the degree of the change of the natural charge value is different for each atom, the value of each atom in the terminal CH<sub>2</sub> region (in the central benzene region) varies toward positive (negative) when  $Q = -2.0$  au versus when  $Q = 0.0$  au, and most of the charge transfer also occurs between C<sub>1</sub> and C<sub>2</sub>, which make the bond between the terminal and central regions (Figure 5). These observations indicate that the external pc induces the nonuniform charge distribution, that is, the D–π–D type ICT from the external methylene region to the central benzene ring in this case, and thus that the present model would be suitable for the investigation of D–π–D type ICT effect. Taking into account the variation in *r* and *Q*, it turns out that the *r* value dependencies of the charge transfer  $-\Delta q$  are smaller than the dependencies of  $-\Delta q$  on the external pc magnitude  $|Q|$  (see Figures S2 and S3 in the Supporting Information). We thus quantify the D–π–D nature as that of the nearly closed-shell PQM-pc system with  $r = 1.35$  Å. Therefore, the present results



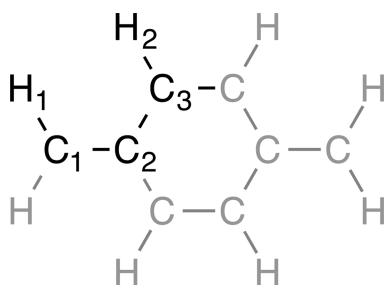


Figure 5. Atom-numbering scheme of symmetric PQM-pc model.

are expected to clarify the effect of introducing D- $\pi$ -D nature on the  $\gamma$  value of the original PQM systems with different diradical characters. We consider the range of the D- $\pi$ -D strength so as to be large enough to describe the real D- $\pi$ -D systems, for example, one of the traditional donor tetra-substituted systems, tetramethoxy-substituted PQM, exhibits an ICT value of about  $-0.30$  au, which is slightly smaller than that ( $-0.45$  au) of the PQM-pc model with  $-1.0$  au pc's. Furthermore, the B-disubstituted PQM, PQM-B2m, which is considered to exhibit quite a large ICT because of the strong point-charge-induced field effect, shows a D- $\pi$ -D nature (ICT =  $-1.05$  au) similar to the PQM-pc model with  $Q = -2.5$  au (ICT =  $-1.11$  au).

**2.4. Calculation of Second Hyperpolarizabilities  $\gamma$ .** We calculate the longitudinal ( $z$ -axis) component of the  $\gamma$  value, which is expected to be a dominant component, using the finite-field (FF) method.<sup>50</sup> Following the previous study on the original PQM model,<sup>11</sup> we employ the unrestricted coupled cluster method including single and double excitations with a perturbative treatment of the triple excitations (UCCSD(T)) using the extended basis set of the 6-31G\*+ $p$  with a diffuse  $p$  exponent of 0.0523 for C atoms and 0.0447 for B atoms<sup>49</sup> for the calculation of the  $\gamma$  value. All calculations were performed using the Gaussian 09 program package<sup>51</sup> except for the geometry optimization using the GAMESS program package.<sup>52</sup>

### 3. RESULTS AND DISCUSSION

**3.1. Diradical Character of the PQM-pc Model.** Figure 6 shows the variation in the diradical character  $y$  of the PQM-pc model as a function of the exocyclic C-C bond length  $r$  for each pc  $Q$ . It was found that all of the systems with and without pc's have similar tendencies for the  $y$  value to increase monotonically as a function of  $r$ , which agrees with those of the

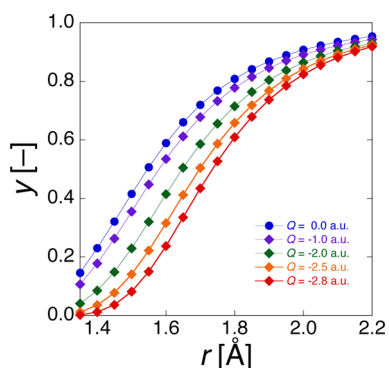


Figure 6. Variation in the diradical character  $y$  with the exocyclic C-C bond length  $r$  for the PQM-pc model with pc's  $Q = 0.0, -1.0, -2.0, -2.5$ , and  $-2.8$  au calculated using the PUHF/6-31G\*+ $p$  method.

original PQM model although the  $y$  value decreases when the pc increases for each  $r$  value. This tendency evokes the result of our recent study that in the asymmetric two-site VCI model, the larger asymmetry relatively increases the ionic configuration and thus decreases the diradical character.<sup>16</sup> This is understood by the fact that although the present system is symmetric, it exhibits the D- $\pi$ -D type nonuniform charge distribution, where the ICT from D groups to the central benzene ring is expected to relatively increase the weight of the ionic configuration.

**3.2. Second Hyperpolarizabilities  $\gamma$  of the PQM-pc Model.** We investigate the effect of the D- $\pi$ -D nature on the relationship between the  $y$  and  $\gamma$  values, that is, the  $y$ - $\gamma$  correlation. As shown in Figure 7, the  $\gamma$  values have bell-shape

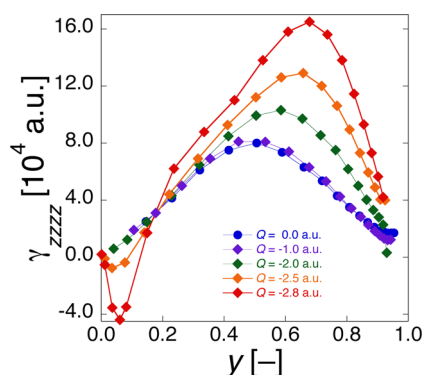
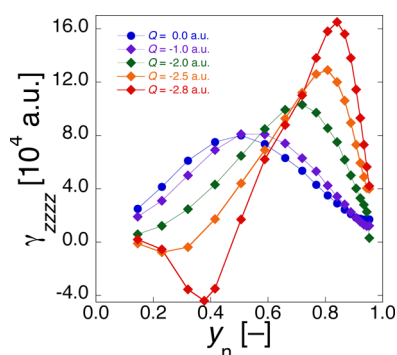


Figure 7. Variation in second hyperpolarizabilities  $\gamma$  as a function of the diradical character  $y$  of the PQM-pc model. The  $y$  and  $\gamma$  values are calculated using the PUHF and UCCSD(T) methods with the 6-31G\*+ $p$  basis set, respectively.

dependencies on the  $y$  values except for the small  $y$  value region with pc's  $Q = -2.5$  and  $-2.8$  au, where the  $\gamma$  values attain negative extrema. The region with negative  $\gamma$  values is predicted to be caused by the larger amplitudes of  $\gamma^{\text{II}}$  (type II contribution with negative sign) compared to those of  $\gamma^{\text{III-2}}$  (type III-2 contribution with positive sign),<sup>53</sup> the feature of which also appears in the quite small  $y$  value region for the symmetric two-site VCI model.<sup>12</sup> These results indicate that regardless of the degree of the D- $\pi$ -D nature, the qualitative  $y$ - $\gamma$  correlation is preserved, that is, the systems with intermediate  $y$  values show large  $\gamma$  values as compared to those of similarly sized closed-shell and pure open-shell systems. Quantitatively, large differences are observed for each  $Q$  series especially on the maximum  $\gamma$  ( $\gamma_{\text{max}}$ ) and the diradical character ( $y_{\text{max}}$ ) giving  $\gamma_{\text{max}}$ . As pc  $Q$  increased, the  $y_{\text{max}}$  and  $\gamma_{\text{max}}$  were found to be enhanced, for example, for pc's  $Q = -2.0, -2.5$ , and  $-2.8$  au,  $(y_{\text{max}}, \gamma_{\text{max}}) = (0.586, 103000 \text{ au}), (0.658, 129000 \text{ au}),$  and  $(0.679, 165000 \text{ au})$ , respectively. The  $\gamma_{\text{max}}$  value for  $Q = -2.8$  au reached about twice as large as that for no pc's. These observations are also similar to the  $y_{\text{A}}$ - $\gamma$  correlation in the asymmetric two-site VCI model with different asymmetry,<sup>16</sup> though the primary virtual excitation process contributing to  $\gamma_{\text{max}}$  ( $\gamma^{\text{III-2}}$ ) in a symmetric system is different from that ( $\gamma^{\text{I}}$ ) in an asymmetric system.

It is also interesting to investigate the correlation between the  $\gamma$  of the PQM-pc model with different pc's  $Q$  and no-point-charge diradical character  $y_{\text{n}}$  of the PQM model with a different  $r$  value from the viewpoint of the molecular design of open-shell singlet D- $\pi$ -D type NLO systems (Figure 8). Using this  $y_{\text{n}}$ - $\gamma$  correlation, we can predict the effect of introducing the



**Figure 8.** Variation in the second hyperpolarizabilities  $\gamma$  as a function of the no-point-charge diradical character  $y_n$ , which represents the diradical character of the PQM model with no pc's. The  $y_n$  and  $\gamma$  values were calculated using the PUHF and UCCSD(T) methods with the 6-31G\*+p basis set, respectively.

D- $\pi$ -D nature on the  $\gamma$  of the PQM systems with different diradical character  $y_n$ .<sup>16</sup> Figure 8 shows that the  $y_{n \max}$  ( $y_n$  value giving  $\gamma_{\max}$ ) moves to the higher  $y_n$  region, for example,  $y_{n \max} = 0.841$  for  $Q = -2.8$  au. It was also found that in the systems with large  $y_n$  values ( $> \sim 0.6$ ), introducing D- $\pi$ -D nature enhances the  $\gamma$  values, while in those with small  $y_n$  values ( $< \sim 0.6$ ), the D- $\pi$ -D nature reduces the  $\gamma$  values. In particular for  $Q = -2.5$  and  $-2.8$  au, negative  $\gamma$  appears in the small  $y_n$  region. This feature suggests that introducing the D- $\pi$ -D nature causes a larger enhancement of the amplitude of the  $\gamma^{\text{II}}$  (negative) contribution than that of the  $\gamma^{\text{III}}$  (positive) contribution in the small  $y_n$  region, while in the large  $y_n$  region, the enhancement of  $\gamma^{\text{III}}$  (positive) contribution significantly exceeds that of  $\gamma^{\text{II}}$  (negative) contribution. Such an effect of the D- $\pi$ -D nature is similar to the asymmetry effect on the  $y$ - $\gamma$  correlation.<sup>16</sup> It was concluded from this behavior that to maximize the effect of introducing the D- $\pi$ -D nature, it would be better to choose the systems with larger  $y$  values as the original systems with uniform charge distribution (no D- $\pi$ -D nature). On the basis of this result, the introduction of strong D groups into the systems with intermediate and nearly pure diradical characters would be a new design guideline for D- $\pi$ -D systems presenting enhanced  $\gamma$  values, which are predicted to be larger than those of conventional closed-shell D- $\pi$ -D systems and of symmetric intermediate diradical systems with uniform charge distribution.

**3.3. B-Disubstituted PQM Dianion Model.** To verify the above result by using a more realistic system, we examine a PQM-B2m model, which is an isoelectronic system to the PQM and is expected to exhibit D- $\pi$ -D nature without any external pc's because of the lower electronegativity of the B atom as well as of two excess electrons. Indeed, the charge distribution of the PQM-B2m model for a fixed exocyclic C-B bond length ( $r = 1.50$  Å), which is almost the same as the equilibrium  $r$  value (1.49 Å), shows that a large ICT occurs from the exocyclic BH<sub>2</sub> region to the central benzene rings and that the natural charge of the central benzene ring is almost equal to that of the PQM-pc model with  $Q = -2.5$  au ( $\Delta q = -1.05$  au (PQM-B2m) and  $-1.11$  au (PQM-pc)). In such a D- $\pi$ -D dianion system, as discussed in section 3.2, decreasing  $y$  values as well as increasing  $\gamma$  values are expected. To clarify the relationship between  $y$  and  $\gamma$ , we investigate the PQM-B2m model by elongating the exocyclic C-B bond. Figure 9 shows the variation in the  $y$  values as a function of the exocyclic X-C bond length  $r$  for the PQM-B2m model ( $X = B$ ) and for the

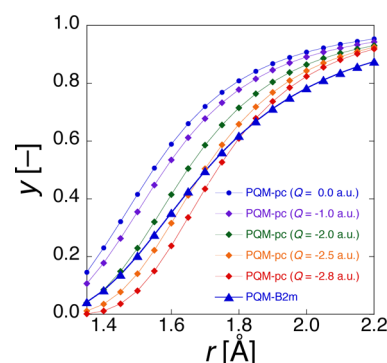


**Figure 9.** Variation in the diradical character  $y$  as a function of the exocyclic X-C bond length  $r$  for the PQM-B2m model ( $X = B$ ) and for the PQM-pc model ( $X = C$ ) calculated using the PUHF/6-31G\*+p method.

PQM-pc model ( $X = C$ ). As expected, it is found that the  $y$  values of the PQM-B2m model are smaller than those of the PQM-pc model with  $Q = 0.0$  au in the whole  $r$  region, and the  $y$  values of PQM-B2m model are located around those of the PQM-pc models with  $Q = -2.0$  to  $-2.8$  au. As previously mentioned, this similarity of the PQM-B2m and PQM-pc models with larger negative pc's originates in the electron distribution of the D- $\pi$ -D nature; that is, the decrease in the  $y$  value stems from the emergence of the significant D- $\pi$ -D nature of the PQM-B2m model.

Concerning the  $\gamma$  values for the PQM-B2m model, we observe the bell-shaped variation of  $\gamma$  as a function of  $y$  as we saw in the case of the PQM-pc model (see Figure 10). On the

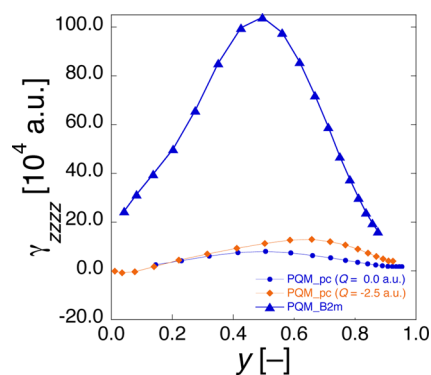


**Figure 10.** Variation in the second hyperpolarizabilities  $\gamma$  as a function of the diradical character  $y$  of the PQM-B2m and PQM-pc ( $Q = 0.0$  and  $-2.5$  au) models. The  $y$  and  $\gamma$  values were calculated using the PUHF and UCCSD(T) methods with the 6-31G\*+p basis set.

other hand, the amplitudes of  $\gamma$  for the PQM-B2m model are about one order larger than those for the PQM-pc models. This remarkable enhancement was speculated to originate in the following three factors. The first factor is the emergence of the D- $\pi$ -D nature in the PQM-B2m model, which is similar to the situation of introducing large pc's  $|Q|$  in the PQM-pc model as shown in section 3.2; however, the enhancement due to the D- $\pi$ -D nature in the neutral state is not so large, for example, the  $\gamma_{\max}$  for the PQM-pc model ( $Q = -2.8$  au) is about twice as large as that of the PQM model. The second factor is the increase in the system size, which could enhance the  $\gamma$  amplitude as shown in the VCI model.<sup>17</sup> It was found from the optimized geometry that the size of the PQM-B2m model is

nearly the same (about 1.03 times) as that of the PQM model for all  $r$  values; for example, for  $r = 1.35$  Å, the exocyclic B–B length for the PQM-B2m model is 2.865 Å and the exocyclic C–C length for the PQM model is 2.789 Å. Even considering the fact that the  $\gamma$  values depend on the fourth power of the effective distances between the radicals within the VCI scheme, the enhancement ratio of  $\gamma$  would be much less than 10. The third factor is the dianionic nature of the PQM-B2m model. In our previous study,<sup>54,55</sup> it was found that the dianionic condensed-ring hydrocarbons exhibit about one order larger  $\gamma$  values than do those of the neutral states, the feature of which is in good agreement with the PQM-B2m results. This is understood by the fact that the B atom has a lower electronegativity than the C atom, and that the present isoelectronic dianionic system possesses two excess electrons loosely bound to the nuclei, which are predicted to significantly enhance the field-induced D– $\pi$ –D type ICT. Namely, the “dianionic state” was found to be the primary origin of enhancing the  $\gamma$  of the PQM-B2m model in the whole diradical character region.

**3.4. A– $\pi$ –A Type ICT Effect on  $y$  and  $\gamma$  Based on the PQM-pc Model.** In the last section, we discuss the A– $\pi$ –A type charge transfer effect in the PQM-pc models with the case of  $Q = +2.0$  au. For the system with positive pc's, it is expected that the ICT with opposite direction, that is, the transfer of the negative charge from the central benzene ring to the terminal CH<sub>2</sub> region, occurs, and as expected, the ICT value  $\Delta q$  is positive for  $Q = +2.0$  au. It turns out that for  $r = 1.35$  Å, the absolute value of  $\Delta q$  is smaller for  $Q = +2.0$  au ( $\Delta q = +0.63$  au) than that for  $Q = -2.0$  au ( $\Delta q = -0.83$  au), probably because of the existence of a small D– $\pi$ –D nature even in the case with no pc ( $\Delta q = -0.12$  au).

Figure 11 shows the variation in the diradical character of the PQM-pc models with pc's of  $\pm 2.0$  au and with no pc. It was

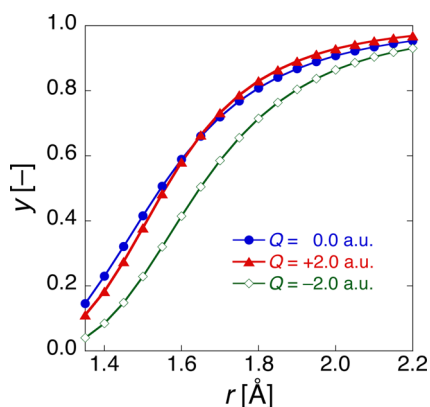


**Figure 11.** Variation in the diradical character  $y$  with the exocyclic C–C bond length  $r$  for the PQM-pc model with pc's  $Q = 0.0$  and  $\pm 2.0$  au calculated using the PUHF/6-31G\*+p method.

found that the  $y$  value for the system with the A– $\pi$ –A type ICT was almost the same as that with no pc, although the D– $\pi$ –D nature decreased  $y$  in the whole  $r$  region. This difference in  $y$  at each  $r$  between the PQM-pc models with positive and negative pc's is explained by the following two factors. One factor is the increase of the ionic configuration in the ICT systems, which is mentioned in section 3.1, in relation to the similarity with the asymmetric VCI model. This factor decreases  $y$  for both the D– $\pi$ –D and A– $\pi$ –A type PQM-pc models. The other factor is the orbital contraction and extension induced by the pc's. For

the PQM-pc model with the D– $\pi$ –D type ICT, the negative pc pushes the electron around the CH<sub>2</sub> region toward the central benzene region, though the opposite effect occurs for the A– $\pi$ –A systems. The latter effect decreases  $y$  for the D– $\pi$ –D systems, while it increases  $y$  for the A– $\pi$ –A systems. It is thus expected that both of these two factors decrease  $y$  for the D– $\pi$ –D type PQM-pc model, even though the two factors work differently on the  $y$  values, while they cancel each other out for the A– $\pi$ –A systems.

The relationship between  $y_n$  and  $\gamma$  is shown in Figure 12. It was found that the maximum  $\gamma$  value of the A– $\pi$ –A systems

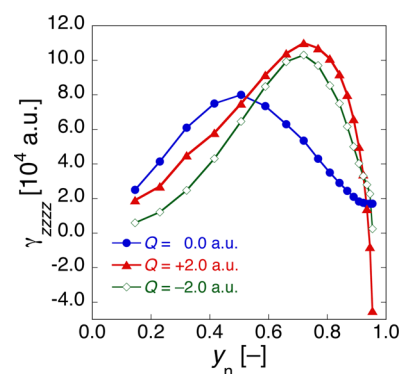


**Figure 12.** Variation in the second hyperpolarizabilities  $\gamma$  as a function of the no-point-charge diradical character  $y_n$ , which represents the diradical character of the PQM model with no pc's. The  $y_n$  and  $\gamma$  values are calculated using the PUHF and UCCSD(T) methods with the 6-31G\*+p basis set, respectively.

shows a similar shift to that of the D– $\pi$ –D systems and that both of the symmetric ICT systems exhibit a similar  $y_n$ – $\gamma$  correlation. It was also found that the tendency of the symmetric ICT effect on the  $y_n$ – $\gamma$  correlation resembles that of the asymmetry effect on the  $y_n$ – $\gamma$  correlation in the VCI model;<sup>16</sup> however, some differences seem to remain in the  $\gamma$  values between the D– $\pi$ –D and A– $\pi$ –A systems. One is that the maximum  $\gamma$  ( $110 \times 10^3$  au) of the A– $\pi$ –A system is larger than that ( $103 \times 10^3$  au) of the D– $\pi$ –D system, though the absolute ICT value of the A– $\pi$ –A system is smaller than that of the D– $\pi$ –D system as previously mentioned. This tendency can also be explained by the increase in the effective distance of the radicals for the A– $\pi$ –A systems. As shown in the previous studies based on the VCI model,<sup>12–16</sup> the  $\gamma$  value has a linear dependence on the fourth power of the effective distance between the radicals. Therefore, the longer effective distance between the radicals is predicted to enlarge the  $\gamma$  value, the feature of which leads to the fact that  $\gamma_{\max}$  of the A– $\pi$ –A system becomes larger than that of the D– $\pi$ –D system. The other difference is that the  $\gamma$  value of the A– $\pi$ –A system in the  $y_n \approx 1$  region falls into large negative values, though that of the D– $\pi$ –D system shows a similar falling except for remaining positive in the present  $y_n$  region. This feature suggests the dominant contribution of type II virtual excitation process ( $\gamma^{\text{II}}$ ) with a negative sign,<sup>53</sup> which is also enhanced in proportion to the fourth power of the effective distance between the radicals.

On the basis of these results, we conclude that the A– $\pi$ –A systems exhibit a similar tendency of the  $\gamma$  value to that of the D– $\pi$ –D systems, though there exist some differences in  $\gamma$  and  $\gamma_{\max}$  because of the orbital extension in the present model systems. These facts show that regardless of the ICT direction,



symmetric ICT gives qualitatively the same effect on the  $\gamma$  value.

#### 4. CONCLUSIONS

The PQM-pc model with different pc's was used to investigate the quadrupole-type ICT effects in the D- $\pi$ -D system on the diradical character  $y$  and the second hyperpolarizabilities  $\gamma$  of open-shell singlet systems. The bell-shaped  $y$ - $\gamma$  correlation was observed in every PQM-pc model as in the case of the PQM model with no pc's. On the other hand, the emergence of the D- $\pi$ -D nature, that is, the quadrupole-type ICT, decreased the  $y$  value and moved the  $y$  value giving the maximum  $\gamma$  to the larger  $y$  region as compared to the case of the PQM model. In addition, the maximum  $\gamma$  value was found to increase with the increase in the D- $\pi$ -D nature. These features were predicted to be related to the large nonuniform charge distribution caused by the ICT in the D- $\pi$ -D system. Indeed, the effects of increasing the D- $\pi$ -D nature on the  $y$ ,  $\gamma$ , and  $y$ - $\gamma$  correlation are shown to be very similar to those of the asymmetry effects on them in the asymmetric diradical system, where the excitation energies and transition properties are found to strongly depend on the asymmetry, that is, the degree of asymmetric ICT.<sup>16</sup> From further analysis on the  $y$ - $\gamma$  correlation, we found a new design guideline for realizing efficient third-order NLO materials composed of the D- $\pi$ -D type open-shell singlet systems: the introduction of the strong D groups into the systems with intermediate and nearly pure diradical characters enhances the  $\gamma$  values as compared to the conventional closed-shell D- $\pi$ -D systems and intermediate symmetric diradical systems with uniform charge distribution.

As a realistic D- $\pi$ -D model, we also investigated the PQM-B2m model, which possesses an isoelectronic structure to the PQM-pc model, though the PQM-B2m is in a dianionic state. We observed similar D- $\pi$ -D nature effects on the  $y$ ,  $\gamma$ , and  $y$ - $\gamma$  correlation to those of the PQM-pc model, while the maximum  $\gamma$  value was about one order larger than that of the PQM-pc model. These results indicate that an appropriate combination of the controlling factors, that is, the intermediate open-shell singlet nature and the strong field-induced ICT nature in the dianionic state of the D- $\pi$ -D system, leads to synergy effects on enhancing  $\gamma$  and thus provide more effective design guidelines for highly efficient third-order NLO systems as compared to the well-known guideline of the quadrupole-type ICT in the closed-shell D- $\pi$ -D system<sup>7-9</sup> and to the later guideline of intermediate singlet diradical systems.<sup>11-25</sup> Further analysis on the A- $\pi$ -A type PQM-pc model has revealed that regardless of the ICT direction, the similar tendency of the  $y$ - $\gamma$  correlation is obtained, the feature of which indicates that the design principles clarified on the D- $\pi$ -D systems are expected to be extended to the A- $\pi$ -A systems. At the next stage, more detailed analysis of the present results, based on the virtual excitation processes, will be performed together with the exploration for more realistic open-shell singlet X- $\pi$ -X (X = D/A) systems.

#### ■ ASSOCIATED CONTENT

##### Supporting Information

Comparison of the intramolecular charge transfers  $-\Delta q$  obtained by several calculation methods, the variation in  $-\Delta q$  for the exocyclic C-C bond length  $r$ , and the justification of the calculation methods. This material is available free of charge via the Internet at <http://pubs.acs.org>.

#### ■ AUTHOR INFORMATION

##### Corresponding Author

\*E-mail: [mnaka@cheng.es.osaka-u.ac.jp](mailto:mnaka@cheng.es.osaka-u.ac.jp), fax: +81-6-6850-6268.

##### Notes

The authors declare no competing financial interest.

#### ■ ACKNOWLEDGMENTS

This work was supported by a Grant-in-Aid for Scientific Research (A) (No. 25248007), a Grant-in-Aid for Scientific Research on Innovative Areas "Stimuli-responsive Chemical Species" (No. A24109002a), MEXT, the Strategic Programs for Innovative Research (SPIRE), and the Computational Materials Science Initiative (CMSI), Japan. Theoretical calculations were partly performed using the Research Center for Computational Science, Okazaki, Japan.

#### ■ REFERENCES

- (1) Tao, S.; Miyagoe, T.; Maeda, A.; Matsuzaki, H.; Ohtsu, H.; Hasegawa, M.; Takaishi, S.; Yamashita, M.; Okamoto, H. Ultrafast Optical Switching by Using Nanocrystals of a Halogen-Bridged Nickel-Chain Compound Dispersed in an Optical Polymer. *Adv. Mater.* **2007**, *19*, 2707-2710.
- (2) Pathenopoulos, D. A.; Rentzepis, P. M. Three Dimensional Optical Storage Memory. *Science* **1989**, *245*, 843-845.
- (3) Zhou, W.; Kuebler, S. M.; Braun, K. L.; Yu, T.; Cammack, J. K.; Ober, C. K.; Perry, J. W.; Marder, S. R. An Efficient Two-Photon-Generated Photoacid Applied to Positive-Tune 3D Microfabrication. *Science* **2002**, *296*, 1106-1109.
- (4) Ehrlich, J. E.; Wu, X. L.; Lee, I.-Y. S.; Hu, Z.-Y.; Röckel, H.; Marder, S. R. Two-Photon Absorption and Broadband Optical Limiting with Bis-Donor Stilbenes. *Opt. Lett.* **1997**, *22*, 1843-1845.
- (5) Frederiksen, P. K.; Jørgensen, M.; Ogilby, P. R. Two-Photon Photosynthesized Production of Singlet Oxygen. *J. Am. Chem. Soc.* **2001**, *123*, 1215-1221.
- (6) Slepko, A. D.; Hegmann, F. A.; Eisler, S.; Elliott, E.; Tykewski, R. R. The Surprising Nonlinear Optical Properties of Conjugated Polyene Oligomers. *J. Chem. Phys.* **2004**, *120*, 6807-6810.
- (7) Albota, M.; Beljonne, D.; Brédas, J.-L.; Ehrlich, J. E.; Fu, J.-Y.; Heikal, A. A.; Hess, S. E.; Koeck, T.; Levin, M. D.; Marder, S. R.; et al. Design of Organic Molecules with Large Two-Photon Absorption Cross Sections. *Science* **1998**, *281*, 1653-1656.
- (8) Rumi, M.; Ehrlich, J. E.; Heikal, A. A.; Perry, J. W.; Barlow, S.; Hu, Z.; McCord-Maughon, D.; Parker, T. C.; Röckel, H.; Thayumanavan, S.; et al. Structure-Property Relationships for Two-Photon Absorbing Chromophores: Bis-Donor Diphenylpolyene and Bis(styryl)benzene Derivatives. *J. Am. Chem. Soc.* **2000**, *122*, 9500-9510.
- (9) Ventelon, L.; Charier, S.; Moreaux, L.; Mertz, J.; Blanchard-Desce, M. Nanoscale Push-Push Dihydrophenanthrene Derivatives as Novel Fluorophores for Two-Photon-Excited Fluorescence. *Angew. Chem., Int. Ed.* **2001**, *40*, 2098-2101.
- (10) Johnston, M. D.; Subbaswamy, K. R.; Senatore, G. Hyperpolarizabilities of Alkali Halide Crystals Using the Local-Density Approximation. *Phys. Rev. B* **1987**, *36*, 9202-9211.
- (11) Nakano, M.; Kishi, R.; Nitta, T.; Kubo, T.; Nakasuji, K.; Kamada, K.; Ohta, K.; Champagne, B.; Botek, E.; Yamaguchi, K. Second Hyperpolarizability ( $\gamma$ ) of Singlet Diradical Systems: Dependence of  $\gamma$  on the Diradical Character. *J. Phys. Chem. A* **2005**, *109*, 885-891.
- (12) Nakano, M.; Kishi, R.; Ohta, S.; Takahashi, H.; Kubo, T.; Kamada, K.; Ohta, K.; Botek, E.; Champagne, B. Relationship between Third-Order Nonlinear Optical Properties and Magnetic Interactions in Open-Shell Systems: A New Paradigm for Nonlinear Optics. *Phys. Rev. Lett.* **2007**, *99*, 033001-1-033001-4.
- (13) Nakano, M.; Kishi, R.; Ohta, S.; Takebe, A.; Takahashi, H.; Furukawa, S.; Kubo, T.; Morita, Y.; Nakasuji, K.; Yamaguchi, K.; et al. Origin of the Enhancement of the Second Hyperpolarizability of



Singlet Diradical Systems with Intermediate Diradical Character. *J. Chem. Phys.* **2006**, *125*, 074113–1–074113–9.

(14) Nakano, M.; Yoneda, K.; Kishi, R.; Takahashi, H.; Kubo, T.; Kamada, K.; Ohta, K.; Botek, E.; Champagne, B. Remarkable Two-Photon Absorption in Open-Shell Singlet Systems. *J. Chem. Phys.* **2009**, *131*, 114316–1–114316–7.

(15) Nakano, M.; Champagne, B.; Botek, E.; Ohta, K.; Kamada, K.; Kubo, T. Giant Electric Field Effect on the Second Hyperpolarizability of Symmetric Singlet Diradical Molecules. *J. Chem. Phys.* **2010**, *133*, 154302–1–154302–15.

(16) Nakano, M.; Champagne, B. Diradical Character Dependences of the First and Second Hyperpolarizabilities of Asymmetric Open-Shell Singlet Systems. *J. Chem. Phys.* **2013**, *138*, 244306–1–244306–13.

(17) Nakano, M.; Minami, T.; Fukui, H.; Kishi, R.; Shigeta, Y.; Champagne, B. Full Configuration Interaction Calculations of the Second Hyperpolarizabilities of the H<sub>4</sub> Model Compound: Summation-Over-States Analysis and Interplay with Diradical Characters. *J. Chem. Phys.* **2012**, *136*, 024315–1–024315–7.

(18) Fukui, H.; Nakano, M.; Shigeta, Y.; Champagne, B. Origin of the Enhancement of the Second Hyperpolarizabilities in Open-Shell Singlet Transition-Metal Systems with Metal–Metal Multiple Bonds. *J. Phys. Chem. Lett.* **2011**, *2*, 2063–2066.

(19) Fukui, H.; Inoue, Y.; Yamada, T.; Ito, S.; Shigeta, Y.; Kishi, R.; Champagne, B.; Nakano, M. Enhancement of the Third-Order Nonlinear Optical Properties in Open-Shell Singlet Transition-Metal Dinuclear Systems: Effects of the Group, of the Period, and of the Charge of the Metal Atom. *J. Phys. Chem. A* **2012**, *116*, 5501–5509.

(20) Matsui, H.; Fukuda, K.; Hirotsaki, Y.; Takamuku, S.; Champagne, B.; Nakano, M. Theoretical Study on the Diradical Characters and Third-Order Nonlinear Optical Properties of Cyclic Thiazyl Diradical Compounds. *Chem. Phys. Lett.* **2013**, *585*, 112–116.

(21) Nakano, M.; Kubo, T.; Kamada, K.; Ohta, K.; Kishi, R.; Ohta, S.; Nakagawa, N.; Takahashi, H.; Furukawa, S.; Morita, Y.; et al. Second Hyperpolarizabilities of Polycyclic Aromatic Hydrocarbons Involving Phenalenyl Radical Units. *Chem. Phys. Lett.* **2006**, *418*, 142–147.

(22) Nakano, M.; Nagai, H.; Fukui, H.; Yoneda, K.; Kishi, R.; Takahashi, H.; Shimizu, A.; Kubo, T.; Kamada, K.; Ohta, K.; et al. Theoretical Study of Third-Order Nonlinear Optical Properties in Square Nanographenes with Open-Shell Singlet Ground States. *Chem. Phys. Lett.* **2008**, *467*, 120–125.

(23) Nagai, H.; Nakano, M.; Yoneda, K.; Kishi, R.; Takahashi, H.; Shimizu, A.; Kubo, T.; Kamada, K.; Ohta, K.; Botek, E.; et al. Signature of Multiradical Character in Second Hyperpolarizabilities of Rectangular Graphene Nanoflakes. *Chem. Phys. Lett.* **2010**, *489*, 212–218.

(24) Yoneda, K.; Nakano, M.; Inoue, Y.; Inui, T.; Fukuda, K.; Shigeta, Y.; Kubo, T.; Champagne, B. Impact of Antidot Structure on the Multiradical Characters, Aromaticities, and Third-Order Nonlinear Optical Properties of Hexagonal Graphene Nanoflakes. *J. Phys. Chem. C* **2012**, *116*, 17787–17795.

(25) Yoneda, K.; Nakano, M.; Fukui, H.; Minami, T.; Shigeta, Y.; Kubo, T.; Botek, E.; Champagne, B. Open-Shell Characters and Second Hyperpolarizabilities of One-Dimensional Graphene Nanoflakes Composed of Trigonal Graphene Units. *ChemPhysChem* **2011**, *12*, 1697–1707.

(26) Hayes, E. F.; Siu, A. K. Q. Electronic Structure of the Open Forms of Three-Membered Rings. *J. Am. Chem. Soc.* **1971**, *93*, 2090–2091.

(27) Yamaguchi, K. In *Self-Consistent Field: Theory and Applications*; Carbo, R., Klobukowski, M., Eds.; Elsevier: Amsterdam, 1990; pp 727–828.

(28) Head-Gordon, M. Characterizing Unpaired Electrons from the One-Particle Density Matrix. *Chem. Phys. Lett.* **2003**, *372*, 508–511.

(29) Kamada, K.; Ohta, K.; Shimizu, A.; Kubo, T.; Kishi, R.; Takahashi, H.; Botek, E.; Champagne, B.; Nakano, M. Singlet Diradical Character from Experiment. *J. Phys. Chem. Lett.* **2010**, *1*, 937–940.

(30) Nakano, M.; Fukui, H.; Minami, T.; Yoneda, K.; Shigeta, Y.; Kishi, R.; Champagne, B.; Botek, E.; Kubo, T.; Ohta, K. (Hyper)polarizability Density Analysis for Open-Shell Molecular Systems Based on Natural Orbitals and Occupation Numbers. *Theor. Chem. Acc.* **2011**, *130*, 711–724 erratum *130*, 725–726.

(31) Lambert, C. Towards Polycyclic Aromatic Hydrocarbons with a Singlet Open-Shell Ground State. *Angew. Chem., Int. Ed.* **2011**, *50*, 1756–1758.

(32) Sun, Z.; Wu, J. Open-Shell Polycyclic Aromatic Hydrocarbons. *J. Mater. Chem.* **2012**, *22*, 4151–4160.

(33) Yasuda, K.; Bhanuprakash, K. Origin of Near-Infrared Absorption and Large Second Hyperpolarizability in Oxyallyl Diradicaloids: A Three-State Model Approach. *J. Phys. Chem. A* **2007**, *111*, 1943–1952.

(34) Li, Z.-J.; Wang, F.-F.; Li, Z.-R.; Xu, H.-L.; Huang, X.-R.; Wu, D.; Chen, W.; Yu, G.-T.; Gu, F.-L.; Aoki, Y. Large Static First and Second Hyperpolarizabilities Dominated by Excess Electron Transition for Radical Ion Pair Salts M<sub>2</sub><sup>+</sup>TCNQ<sup>−</sup> (M = Li, Na, K). *Phys. Chem. Chem. Phys.* **2009**, *11*, 402–408.

(35) Jha, P. C.; Rinkevicius, Z.; Ågren, H. Spin Multiplicity Dependence of Nonlinear Optical Properties. *ChemPhysChem* **2009**, *10*, 817–823.

(36) Serrano-Andrés, L.; Avramopoulos, A.; Li, J.; Labéguerie, P.; Bégue, D.; Kellö, V.; Papadopoulos, M. G. Linear and Nonlinear Optical Properties of a Series of Ni-Ditholene Derivatives. *J. Chem. Phys.* **2009**, *131*, 134312–1–134312–11.

(37) He, G. S.; Zhu, J.; Baev, A.; Samoć, M.; Frattarelli, D. L.; Watanabe, N.; Facchetti, A.; Ågren, H.; Marks, T. J.; Prasad, P. N. Twisted  $\pi$ -System Chromophores for All-Optical Switching. *J. Am. Chem. Soc.* **2011**, *133*, 6675–6680.

(38) Zhong, R.-L.; Zhang, J.; Muhammad, S.; Hu, Y.-Y.; Xu, H.-L.; Su, Z.-M. Boron/Nitrogen Substitution of the Central Carbon Atoms of the Biphenalenyl Dimer: A Novel 2e-12c bond and Large NLO Responses. *Chem.—Eur. J.* **2011**, *17*, 11773–11779.

(39) Ishida, M.; Shin, J.-Y.; Lim, J.-M.; Lee, B.-S.; Yoon, M.-C.; Koide, T.; Sessler, J.-L.; Osuka, A.; Kim, D. Neutral Radical and Singlet Biradical Forms of Meso-Free, -Keto and -Diketo Hexaphyrins(1.1.1.1.1.1): Effects on Aromaticity and Photophysical Properties. *J. Am. Chem. Soc.* **2011**, *133*, 15533–15544.

(40) Kamada, K.; Ohta, K.; Kubo, T.; Shimizu, A.; Morita, Y.; Nakasui, K.; Kishi, R.; Ohta, S.; Furukawa, S.; Takahashi, H.; et al. Strong Two-Photon Absorption of Singlet Diradical Hydrocarbons. *Angew. Chem., Int. Ed.* **2007**, *46*, 3544–3546.

(41) Zeng, Z.; Sung, Y. M.; Bao, N.; Tan, D.; Lee, R.; Zafra, J. L.; Lee, B. S.; Ishida, M.; Ding, J.; Navarrete, J. T. L.; et al. Stable Tetrabenzo-Chichibabin's Hydrocarbons: Tunable Ground State and Unusual Transition between Their Closed-Shell and Open-Shell Resonance Forms. *J. Am. Chem. Soc.* **2012**, *134*, 14513–14525.

(42) Li, Y.; Heng, W. K.; Lee, B. S.; Aratani, N.; Zafra, J. L.; Bao, N.; Lee, R.; Sung, Y. M.; Sun, Z.; Huang, K. W.; et al. Kinetically Blocked Stable Heptazethrene and Octazethrene: Closed-Shell or Open-Shell in the Ground State? *J. Am. Chem. Soc.* **2012**, *134*, 14913–14932.

(43) Kamada, K.; Fuku-en, S.-I.; Minamide, S.; Ohta, K.; Kishi, R.; Nakano, M.; Matsuzaki, M.; Okamoto, H.; Higashikawa, H.; Inoue, K.; et al. Impact of Diradical Character on Two-Photon Absorption: Bis(acridine) Dimers Synthesized from an Allenic Precursor. *J. Am. Chem. Soc.* **2013**, *135*, 232–241.

(44) Zeng, Z.; Lee, S.; Zafra, J. L.; Ishida, M.; Zhu, X.; Sun, Z.; Ni, Y.; Webster, R. D.; Li, R.-W.; López Navarrete, J. T.; et al. Tetracyanoquaterylene and Tetracyanohexarylenequinodimethanes with Tunable Ground States and Strong Near-Infrared Absorption. *Angew. Chem., Int. Ed.* **2013**, *52*, 8561–8565.

(45) Kishida, H.; Hibino, K.; Nakamura, A.; Kato, D.; Abe, J. Third-Order Nonlinear Optical Properties of a  $\pi$ -Conjugated Biradical Molecule Investigated by Third-Harmonic Generation Spectroscopy. *Thin Solid Films* **2010**, *519*, 1028–1030.

(46) Takauji, K.; Suizu, R.; Awaga, K.; Kishida, H.; Nakamura, A. Third-Order Nonlinear Optical Properties and Electroabsorption

Spectra of an Organic Biradical, [Naphtho[2,1-*d*:6,5-*d'*]bis([1,2,3]-dithiazole)]. *J. Phys. Chem. C* **2014**, *118*, 4303–4308.

(47) Shao, Y.; Head-Gordon, M.; Krylov, A. I. The Spin-Flip Approach within Time-Dependent Density Functional Theory: Theory and Applications to Diradicals. *J. Chem. Phys.* **2003**, *118*, 4807–4818.

(48) Kishi, R.; Nakano, M.; Ohta, S.; Takebe, A.; Nate, M.; Takahashi, H.; Kubo, T.; Kamada, K.; Ohta, K.; Champagne, B.; et al. Finite-Field Spin-Flip Configuration Interaction Calculation of the Second Hyperpolarizabilities of Singlet Diradical Systems. *J. Chem. Theory Comput.* **2007**, *3*, 1699–1707.

(49) de Wergifosse, M.; Wautelet, F.; Champagne, B.; Kishi, R.; Fukuda, K.; Matsui, H.; Nakano, M. Challenging Compounds for Calculating Hyperpolarizabilities: *p*-Quinodimethane Derivatives. *J. Phys. Chem. A* **2013**, *117*, 4709–4715.

(50) Cohen, H. D.; Roothaan, C. C. Electric Dipole Polarizability of Atoms by the Hartree-Fock Method. I. Theory for Closed-Shell Systems. *J. Chem. Phys.* **1965**, *43*, S34–S39.

(51) Frisch, M. J.; Trucks, G. W.; Schlegel, H. B.; Scuseria, G. E.; Robb, M. A.; Cheeseman, J. R.; Scalmani, G.; Barone, V.; Mennucci, B.; Petersson, G. A.; Nakatsuji, H.; Caricato, M.; Li, X.; Hratchian, H. P.; Izmaylov, A. F.; Bloino, J.; Zheng, G.; Sonnenberg, J. L.; Hada, M.; Ehara, M.; Toyota, K.; Fukuda, R.; Hasegawa, J.; Ishida, M.; Nakajima, T.; Honda, Y.; Kitao, O.; Nakai, H.; Vreven, T.; Montgomery, J. A., Jr.; Peralta, J. E.; Ogliaro, F.; Bearpark, M.; Heyd, J. J.; Brothers, E.; Kudin, K. N.; Staroverov, V. N.; Kobayashi, R.; Normand, J.; Raghavachari, K.; Rendell, A.; Burant, J. C.; Iyengar, S. S.; Tomasi, J.; Cossi, M.; Rega, N.; Millam, J. M.; Klene, M.; Knox, J. E.; Cross, J. B.; Bakken, V.; Adamo, C.; Jaramillo, J.; Gomperts, R.; Stratmann, R. E.; Yazyev, O.; Austin, A. J.; Cammi, R.; Pomelli, C.; Ochterski, J. W.; Martin, R. L.; Morokuma, K.; Zakrzewski, V. G.; Voth, G. A.; Salvador, P.; Dannenberg, J. J.; Dapprich, S.; Daniels, A. D.; Farkas, O.; Foresman, J. B.; Ortiz, J. V.; Cioslowski, J.; Fox, D. J. *Gaussian 09*, revision A.02; Gaussian, Inc.: Wallingford, CT, 2009.

(52) Schmidt, M. W.; Baldridge, K. K.; Boatz, J. A.; Elbert, S. T.; Gordon, M. S.; Jensen, J. H.; Koseki, S.; Matsunaga, H.; Nguyen, K. A.; Su, S. J.; et al. General Atomic and Molecular Electronic Structure System. *J. Comput. Chem.* **1993**, *14*, 1347–1363.

(53) Nakano, M.; Yamaguchi, K. A Proposal of New Organic Third-Order Nonlinear Optical Compounds. Centrosymmetric Systems with Large Negative Third-Order Hyperpolarizabilities. *Chem. Phys. Lett.* **1993**, *206*, 285–292.

(54) Nakano, M.; Kiribayashi, S.; Yamada, S.; Shigemoto, I.; Yamaguchi, K. Theoretical Study of the Second Hyperpolarizabilities of Three Charged States of Pentalene. A Consideration of the Structure–Property Correlation for the Sensitive Second Hyperpolarizability. *Chem. Phys. Lett.* **1996**, *262*, 66–73.

(55) Nakano, M.; Yamaguchi, K. Theoretical Studies for Third-Order Hyperpolarizabilities of Alternant and Condensed-Ring Conjugated Systems I. *Mol. Cryst. Liq. Cryst.* **1994**, *255*, 139–148.